Accurate Quasi-Static Model for Conductor Loss in Coplanar Waveguide

M. Saiful Islam, Emre Tuncer, and Dean P. Neikirk
Department of Electrical & Computer Engineering
The University of Texas at Austin
Austin, Texas 78712

Abstract

A quasi-static model for coplanar waveguide (CPW) including conductor loss has been developed. Comparison between experimental measurements on low-loss dielectric substrates and model calculations show excellent agreement. To model the conductor loss, the CPW is conformally-mapped into a parallel plate configuration, where current crowding and conductor loss are accounted for using scaled conductance.

The evaluation of conductor loss remains one of the more difficult problems in transmission line analysis. Traditional approaches such as the incremental inductance rule give poor agreement with experimental results for small dimension (micron size) interconnects. One difficulty with most of these techniques is their failure to adequately model the transition form low frequency to high frequency behavior. When modeling the propagation of broad bandwidth time-domain pulses, such as in digital systems, the dispersion induced by this transition can be very significant. Thus, there is a need for models which accurately predict both the attenuation and phase constants for transmission lines using conductors with finite conductivity.

These problems are especially acute in planar transmission lines, such as coplanar waveguide. Current crowding at the edges of the conductors can lead to a significant increase in ohmic losses. In this paper, we show a quasi-static technique based on conformal mapping which provides excellent agreement between modeled and measured conductor loss over a wide range of dimensions and metal thicknesses. The technique requires no fitting parameters: given the dimensions, metal conductivity, and substrate dielectric constant, the complex propagation constant can be accurately predicted.

Quasi-static analysis, in particular the use of conformal mapping, is well established as a useful technique for the calculation of propagation constants of quasi-TEM transmission lines. The application of conformal mapping to the calculation of the complex internal impedance of conductors is less well known. Collin uses a conformal mapping technique to obtain the high frequency current distribution in CPW, but then uses a standard perturbation technique to approximate the ohmic loss [1].

Here we use the conformal mapping technique to find not only the normal capacitance per unit length of the transmission line, but also to find the frequency dependence of the series inductance and resistance. In general, consider a conformal map $w(z)$ (where $z = x + jy$ is the domain containing the original transmission line) which produces parallel plates in the $w(u, v)$ mapped plane, with the plates parallel to u -axis, extending from 0 to u_o, the top plate located at v_t, and the bottom plate at v_b. The scale factor M relating a differential length in the z-plane to one in the w-plane is just the magnitude of the total derivative of the mapping function:

$$M(u,v)=\left|\frac{dw}{dz}\right|_{u,v} \tag{1}$$

If the conductors in the original domain are much thinner than their lateral extent, they can be approximated as thin sheets with surface resistance R_S given by [2]

$$R_S(\omega)=\mathbf{Re}\left[\frac{\sqrt{\frac{\omega\mu_o}{2\sigma}}(1+j)}{2\tanh\left\{\sqrt{\frac{\omega\mu_o\sigma}{2}}\left(\frac{t}{2}\right)(1+j)\right\}}\right] \tag{2}$$

where t is the thickness and σ the conductivity of the conductors. This surface resistance can be transformed into the mapped domain using the scale factor $M(u, v)$, as illustrated in Fig. 1. The series impedance δZ due to a differential width du of the plates is then just the series combination of the mapped surface resistance and the parallel plate inductance:

$$\delta Z=\frac{R_S\{M(u,v_t)+M(u,v_b)\}}{du}+\frac{j\omega\mu_o|v_t-v_b|}{du} \tag{3}$$

The total series impedance per unit length, including the impact of finite resistance, is then found from the parallel combination of the impedances of each differential width of the plates:

$$Z(\omega)=\left[\int_0^{u_o}\frac{du}{j\omega\mu_o|v_t-v_b|+R_S\{M(u,v_t)+M(u,v_b)\}}\right]^{-1} \tag{4}$$

At low frequencies this reduces to

$$Z=R_{dc}+j\omega\mu_o|v_t-v_b|\left(\frac{R_{dc}}{R_S}\right)^2\int_0^{u_o}\frac{du}{\left[M(u,v_t)+M(u,v_b)\right]^2} \tag{5}$$

where R_{dc} is the dc resistance of the original conductors. At high frequencies eq. 3 becomes

$$Z=\frac{R_S}{u_o^2}\left\{\int_0^{u_o}du\left[M(u,v_t)+M(u,v_b)\right]\right\}+j\omega L_{ext} \tag{6}$$

where L_{ext} is the normal external inductance of the line (given

OF2

CH3277-1/93/0000-0959$01.00 © 1993 IEEE

by $L_{ext} = \frac{\mu_o |v_t - v_b|}{u_o}$ in the mapped domain).

Results & Discussions

To verify the accuracy of this technique measurements have been made on coplanar waveguide fabricated on low loss dielectric substrates. Two different dielectric substrates, semi-insulating GaAs and glass (Pyrex) were used for rf measurements from 45 MHz to 40 GHz. Two different metallization were also used, 0.8 μm of evaporated silver on top of GaAs substrate, and 0.8 μm of electro-plated gold on the Pyrex sample. The CPW dimensions are shown in Fig. 2. The conformal mapping functions discussed in [3, 4] were used in eq. 3.

Both the experimental and the simulated results from our model are shown in Figs. 3 and 4. For the experimental results, attenuation and effective refractive index ($n_{eff} = \beta/\beta_o$) were extracted from the S-parameters measured by an HP 8510B Network Analyzer. Excellent agreement between the experimental results and the calculations for both samples over the full frequency range (45 MHz - 40 GHz) was obtained. Also shown in Fig. 3 and 4 are the calculated attenuation constants from existing quasi-static conductor loss analysis [1]. Other quasi-static analysis from [5], as well as a numerical incremental inductance calculation [6], also failed to match the experimental measurements. The effective resistance (the real part of eq. 4) and inductance (from the imaginary part of eq. 4) calculated from our model for these two structures are shown in Figs. 5 and 6.

To further verify the applicability of this technique, we have also compared the extensive experimental data of Haydl *et al.* [7, 8] to our model; in all cases excellent agreement has been obtained. Figures 7 and 8 show typical comparisons between their results and our calculations over a wide range of CPW dimensions. Again, no fitting factors are used; only the dimensions of the CPW and conductivity of the metal are required for the calculation.

In summary, we have demonstrated a quasi-static technique for the calculation of conductor loss in CPW which shows excellent agreement with experimental measurements. The technique is numerically efficient, and can be readily applied to other planar transmission line structures.

Acknowledgments: This work was sponsored in part by the Joint Services Electronics Program under grant number AFOSR 49620-89-C-0044, and by the Defense Advanced Research Projects Agency Application Specific Electronic Module program.

References

1. R. E. Collin, *Foundations for Microwave Engineering*, 2nd ed., New York, McGraw-Hill, 1992, pp. 898-910.
2. S. Ramo, J. R. Whinnery, and Van T. Duzer, *Fields and Waves in Communication Electronics,* 2nd ed., New York, Wiley, 1984.
3. C. P. Wen, "Coplanar waveguide : A surface strip transmission line suitable for nonreciprocal gyromagnetic device applications," *IEEE Trans. Microwave Theory Tech.*, vol. MTT-17, no. 12, Dec. 1969, pp. 1087-1088.
4. S. M. Wentworth, D. P. Neikirk, and C. R. Brahce, "The high frequency characteristics of Tape Automated Bonding (TAB) interconnects," *IEEE Trans. Components, Hybrids, and Manufacturing Tech.*, vol. 12, no. 3, Sept. 1989, pp. 340-347.
5. K. C. Gupta, R. Garg, I. J. Bahl, *Microstrip Lines and Slotlines*, Norwood, MA : Artech House Inc., 1979, pp. 287.
6. H. Wheeler, "Transmission-Line Properties of a Strip on a Dielectric Sheet on a Plane," *IEEE Trans. Microwave Theory Tech.*, vol. MTT-25, Aug. 1977, pp. 631-647.
7. W. H. Haydl, J. Braunstein, T. Kitazawa, M. Schlechtweg, P. Tasker, L. F. Eastman, "Attenuation of millimeterwave coplanar lines on Gallium Arsenide and Indium Phosphide over the range of 1-60 GHz," *IEEE MTT-S Int. Microwave Symp. Dig.*, June 1991, pp. 349-352.
8. W. H. Haydl, "Experimentally observed frequency variation of the attenuation of millimeterwave coplanar transmission lines with thin metallization," *IEEE Microwave and Guided Wave Lett.*, vol. 2, no. 8, Aug. 1992, pp. 322-324.

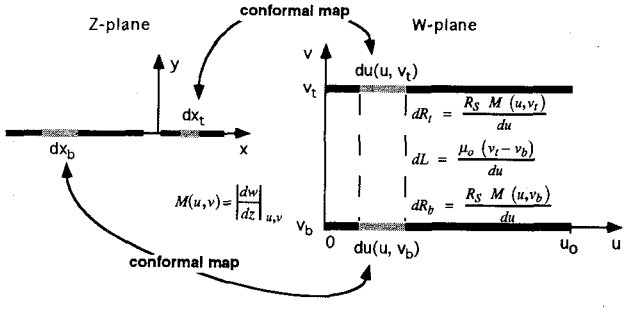

Figure 1: Diagram illustrating use of a conformal map to find the series impedance of a transmission line including the effect of finite resistance.

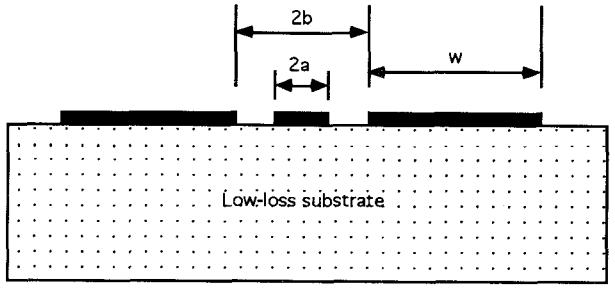

Figure 2: Cross-sectional view of CPW. Dimensions used for semi-insulating GaAs and Pyrex samples are a = 5 μm, b = 12 μm, w = 500 μm.

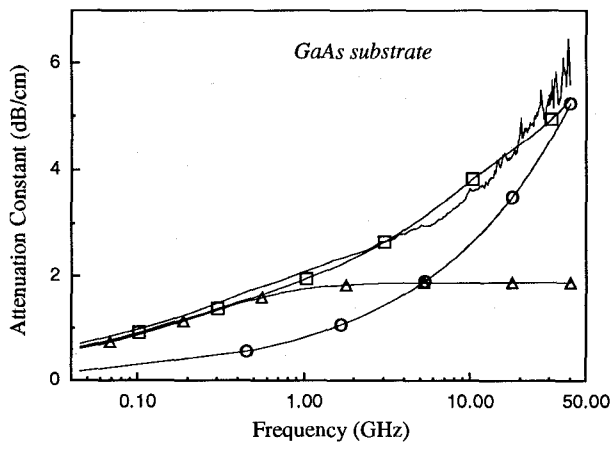

Figure 3: Comparison between measured and calculated attenuation constant on semi-insulating GaAs substrate. CPW dimensions are: a = 5 μm, b = 12 μm, w = 500 μm, t = 0.8 μm, and $\sigma = 6.0 \times 10^5$ S·cm^{-1} (evaporated silver). □: new model, attenuation constant; O: Collin [1], attenuation constant; Δ: attenuation constant assuming constant dc resistance.

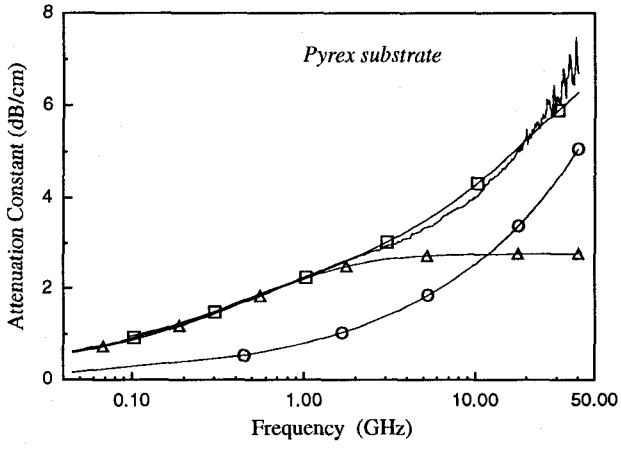

Figure 4: Comparison between measured and calculated attenuation constant on Pyrex (glass) substrate. CPW dimensions are: a = 5 μm, b = 12 μm, w = 500 μm, t = 0.8 μm, and $\sigma = 2.55 \times 10^5$ S·cm^{-1} (electroplated gold). □: new model, attenuation constant; O: Collin [1], attenuation constant; Δ: attenuation constant assuming constant dc resistance.

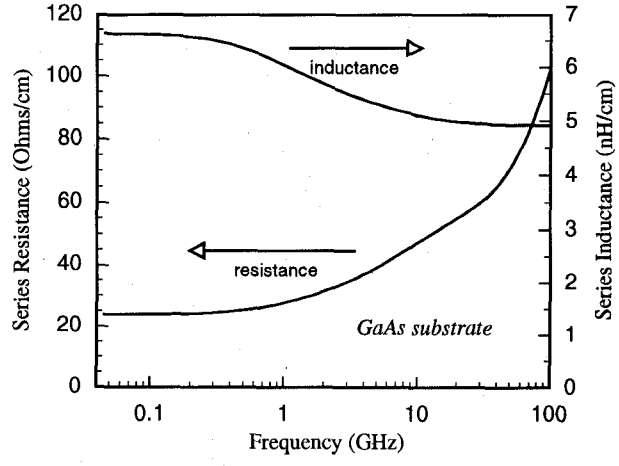

Figure 5: Calculated effective series resistance and inductance on semi-insulating GaAs substrate. CPW dimensions are: a = 5 μm, b = 12 μm, w = 500 μm, t = 0.8 μm, and $\sigma = 6.0 \times 10^5$ S·cm^{-1} (evaporated silver).

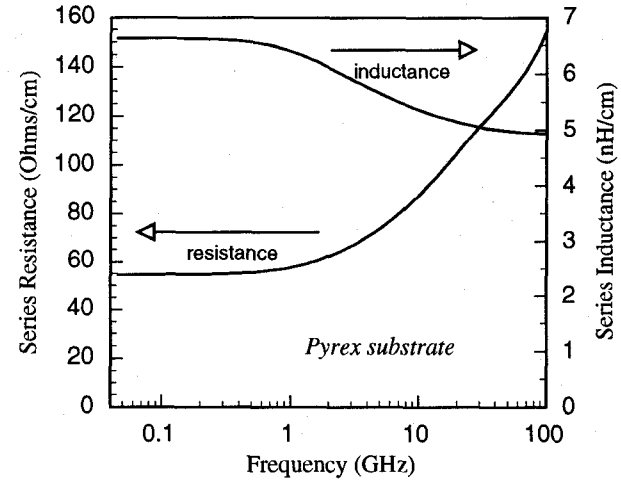

Figure 6: Calculated effective series resistance and inductance on Pyrex (glass) substrate. CPW dimensions are: a = 5 μm, b = 12 μm, w = 500 μm, t = 0.8 μm, and $\sigma = 2.55 \times 10^5$ S·cm^{-1} (electroplated gold).

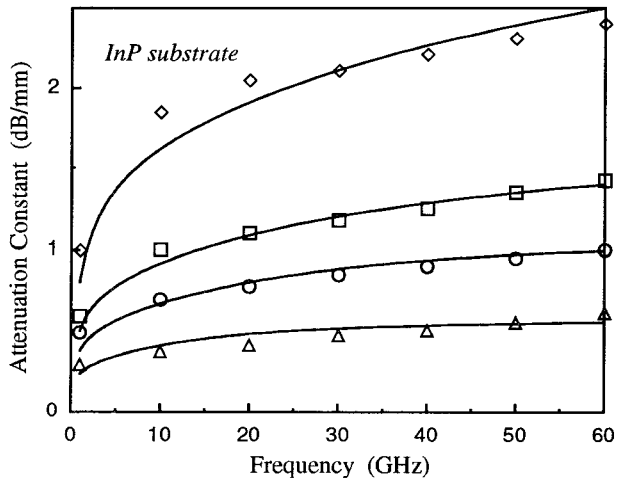

Figure 7: Comparison between the model calculations and experimental results of ref. [7]. Solid lines represent the model data, whereas scattered points are experimental results. CPW dimensions: ◇: a = 2 μm, b = 15 μm, and t = 0.25 μm; □: a = 2 μm, b = 15 μm, and t = 0.5 μm; O: a = 6 μm, b = 45 μm, and t = 0.25 μm; Δ: a = 6 μm, b = 45 μm, and t = 0.5 μm.

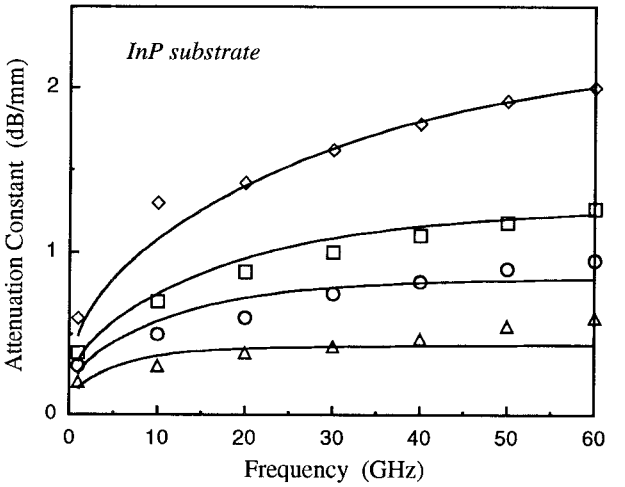

Figure 8: Comparison between the model calculations and experimental results of ref. [7]. Solid lines represent the model data, whereas scattered points are experimental results. CPW dimensions: ◇: a = 11 μm, b = 15 μm, and t = 0.25 μm; □: a = 11 μm, b = 15 μm, and t = 0.5 μm; O: a = 33 μm, b = 45 μm, and t = 0.25 μm; Δ: a = 33 μm, b = 45 μm, and t = 0.5 μm.